1 January 2000

Optics Communications 173 (2000) 333–340

OPTICS COMMUNICATIONS

www.elsevier.com/locate/optcom

Gain and absorption saturation coupling in end pumped $Tm:YVO_4$ and Tm,Ho:YLF CW amplifiers

Gilbert L. Bourdet *

Laboratoire d'Optique Appliquée, Ecole Polytechnique – Ecole Nationale Supérieure de Techniques Avancées, Centre National de la Recherche Scientifique, Unité Mixte de Recherche 7639, Chemin de la Hunière, F-91761 Palaiseau Cedex, France

Received 8 July 1999; received in revised form 7 October 1999; accepted 12 October 1999

Abstract

In this paper we theoretically investigate the coupling between gain and absorption saturation in quasi three level CW longitudinally pumped amplifier exhibiting up-conversion and ground state depletion. Numerical computations are performed for both $Tm:YVO_4$ and Tm,Ho:YLF crystals. We show that the absorption of the pump strongly increases with increasing intensity of the amplified wave. We also investigate the effect of the up-conversion process and we find that, at high laser intensity level, quite comparable results are found with and without up-conversion. Last, we investigate the round trip amplification of a low intensity laser beam when both the laser and the pump beams are Gaussian and we analyse the amplified beam shape as a function of the ratio of the pump and the laser beam waist size.

1. Introduction

Several investigations have been devoted to quasi three level diode pumped lasers that make possible to set up high efficient all solid state lasers emitting in the eye safe spectral range. These include erbium for low altitude laser range finding and optical fibers communications [1,2], thulium, holmium or codoped thulium–holmium for medical applications [3], coherent Doppler LIDAR wind sensing, wind shear detection, differential absorption LIDAR (DIAL) water profiling and ranging [4–9]. These systems suffer from a reduction of both the absorption rate due to the ground state depletion and the gain due to the upper laser level depopulation resulting from up-conversion under intense pumping. In addition, as the lower laser level is thermally populated at room temperature, the laser wave may be reabsorbed. An accurate model taking into account these processes has already been described [8] and theoretical modelling in good agreement with experimental results has been set up for $Tm:YVO_4$ [9] and Tm,Ho:YLF [10] end pumped microchip lasers. Using these models, we now investigate the dependence of the absorption of the pump wave with the amplification of the laser wave. We show that, when the intensity of the amplified wave is large, pump absorption is increased as a result of the repopulation of the ground state level by stimulated emission and that up-conversion has negligible effect in these conditions.

* Tel.: +33-1-6931-9996; e-mail: bourdet@enstay.ensta.fr

PII: S0030-4018(99)00618-5

2. Tm:YVO$_4$ amplifier

Fig. 1 presents the lowest energy manifolds for Tm^{3+} involved in the laser process. In CW regime, we have shown [9] that the amplification of the laser wave and the absorption of the pump wave may be described by:

$$\frac{\mathrm{d}I_\mathrm{l}^\varepsilon}{I_\mathrm{l}^\varepsilon} = \varepsilon g_0 \{ X_2 - f \} \,\mathrm{d}z,$$

$$\frac{\mathrm{d}I_\mathrm{p}^{\varepsilon'}}{I_\mathrm{p}^{\varepsilon'}} = -\varepsilon' \alpha_0 \{ 1 - X_2 \} \,\mathrm{d}z \tag{1}$$

where $\varepsilon = \pm 1$ for the laser and $\varepsilon' = \pm 1$ for the pump ($\pm$ for the upper index of I_i^ε) refer to the direction of propagation of the laser and the pump waves, I_i^ε is the laser ($i = \mathrm{l}$) and the pump ($i = \mathrm{p}$) intensity normalized to their saturation intensities, and:

$$X_2 = \frac{N_2}{N_\mathrm{Tm}}, \quad g_0 = \sigma_1 N_\mathrm{Tm} (f_\mathrm{u} + f_\mathrm{l}),$$

$$\alpha_0 = \sigma_\mathrm{p} N_\mathrm{Tm}, \quad f = \frac{f_\mathrm{l}}{f_\mathrm{u} + f_\mathrm{l}} \tag{2}$$

where σ_i is the laser emission ($i = \mathrm{l}$) and pump absorption ($i = \mathrm{p}$) cross-section, N_Tm is the thulium doping concentration, N_2 is the upper level population density, and f_j is the Boltzmann factor for the upper ($j = \mathrm{u}$) and the lower ($j = \mathrm{l}$) level of the lasing transition. In CW operation, the rate equation system reduces to a single equation making then possible to compute X as a function of the laser and pump wave intensities [8]:

$$X_2 = \frac{\sqrt{\left(1 + I_\mathrm{p} + I_\mathrm{l}\right)^2 + 2b\left(I_\mathrm{p} + fI_\mathrm{l}\right)} - \left(1 + I_\mathrm{p} + I_\mathrm{l}\right)}{b} \tag{3}$$

where I_i is the sum of the intensity for the waves travelling in both directions for the pump ($i = \mathrm{p}$) and the laser ($i = \mathrm{l}$) light normalized to their saturation intensities, and b is the total up-conversion loss parameter defined in [8]. Combining the equations in (1), one can obtain relations connecting the pump and laser intensities travelling in both directions:

$$I_\mathrm{l}^+(z)\, I_\mathrm{l}^-(z) = C_\mathrm{l}, \quad I_\mathrm{p}^+(z)\, I_\mathrm{p}^-(z) = C_\mathrm{p} \tag{4a}$$

Furthermore, by eliminating X in the Eq. (1), we get:

$$\frac{1}{\varepsilon g_0} \frac{\mathrm{d}I_\mathrm{l}^\varepsilon}{I_\mathrm{l}^\varepsilon} = \frac{1}{\varepsilon' \alpha_0} \frac{\mathrm{d}I_\mathrm{p}^{\varepsilon'}}{I_\mathrm{p}^{\varepsilon'}} + (1 - f)\,\mathrm{d}z$$

leading to:

$$I_\mathrm{l}^\varepsilon(z) = C_{\varepsilon\varepsilon'} \left\{ I_\mathrm{p}^{\varepsilon'}(z) \right\}^{\varepsilon\varepsilon' D} \mathrm{e}^{\varepsilon \delta z} \tag{4b}$$

with

$$D = \frac{g_0}{\alpha_0}, \quad \delta = g_0 (1 - f) \tag{5}$$

and C_l, C_p and $C_{\varepsilon\varepsilon'}$ are constants we can calculate using the boundary conditions. Using the parameters of a 5% Tm:YVO$_4$ crystal at room temperature:

$$g_0 = 0.41\ \mathrm{cm}^{-1}, \quad \alpha_0 = 32\ \mathrm{cm}^{-1}$$

$$f = 0.335, \quad b = 2$$

we compute the gain and the transmission for a 1 mm long amplifier crystal. We note that the intensities are normalised to the saturation intensities for the laser and the pump, respectively:

$$I_\mathrm{sat}^\mathrm{l} = 188\ \mathrm{kW/cm^2}, \quad I_\mathrm{sat}^\mathrm{p} = 2.99\ \mathrm{kW/cm^2}$$

In Fig. 3 the saturation of the transmission of the crystal appears when the injected laser wave increases from 0 to 80 in steps of 5. With no injected laser wave, the transmission is as high as 92% and

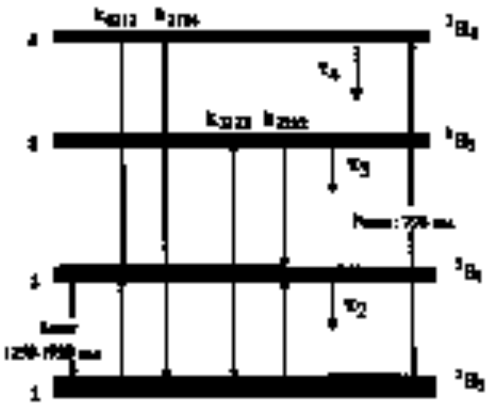

Fig. 1. Diagram of the four lowest Tm^{3+} energy manifolds and atomic transitions.

reduces to 22% for an injected laser intensity equal to 80. This behaviour has already been observed [4].

For these simulations, we have used an active mirror configuration in which the pump is launched by means of a dichroic mirror that reflects the pump wave and transmits the laser wave and where the crystal is cooled by the rear face that reflects both the pump and the laser waves (R has been set equal to 0.995 for the computations) [9,10]. In Fig. 2 is plotted the round trip gain versus the injected laser wave intensity $I_{las}(0)$ for various levels of the launched pump intensity $I_{pump}(0)$ ranging from 0 to 80 in steps of 5. For low pumping level ($X < f$), the crystal absorbs the injected laser wave. By increasing the pump intensity, the gain at low input signal increases fast in a first time and saturates for $I_{pump}(0) > 8$. This behaviour is shown in Fig. 3 (curve A) where the gain is plotted versus the pump intensity for a low injected laser intensity $I_{las}(0) = 10^{-4}$. Nevertheless, the laser intensity required for a 3 dB reduction of the small signal gain (Fig. 3 curve B) increases with the pump intensity. In Fig. 4 the reflection saturation appears showing that it reduces from 91% with no injected laser wave down to 3% for $I_{las}(0) = 80$. This behaviour has already been observed [4]. Similar computation with no up-conversion ($b \to 0$) shows that neither the gain (Fig. 3 dashed line) nor the absorption change appreciably in the range of pump and laser intensity hereby investigated.

In [9], for a Tm:YVO_4 microchip laser 1 mm long, the launched pump intensity is about 70 at the

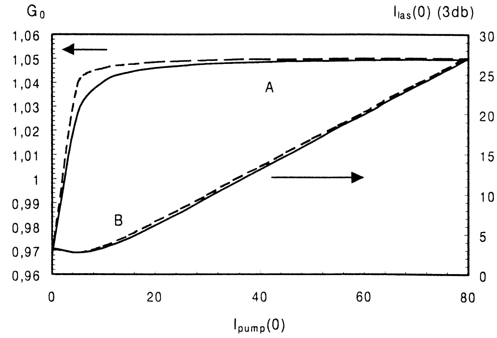

Fig. 3. Saturation of the small signal round trip gain (curve A) and input laser intensity required for a 3 dB reduction (curve B) versus the input pump intensity with (solid line) and without (dashed line) up-conversion.

top of the pump beam. The corresponding laser wave intensity reflected by the front face mirror 98% in reflectivity is 25. With regards to the results shown in Fig. 4, the corresponding reflected pump intensity is 16%. This is in good agreement with the results presented in [9] for which a residual reflectivity of the front face mirror at the pump wavelength of 18% leads to a large amount of the launched pump power stored inside the laser cavity and then, a very low reflected pump power. Using Fig. 4, it is also possible to determine the output intensity as a function of the front face reflectivity at the laser wavelength. The oscillation condition reads:

$$GR_{out} = 1$$

where G is the round trip saturated gain, and R_{out} is

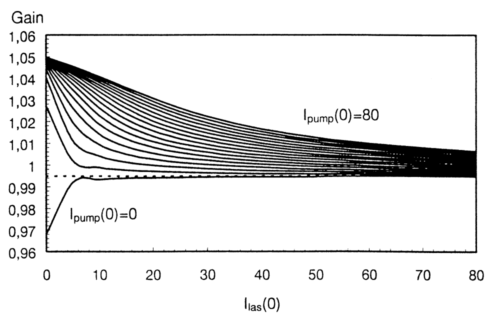

Fig. 2. Saturation of the round trip gain versus the input laser intensity for the input pump intensity varying in steps of 5. The YVO_4 crystal length is 1 mm.

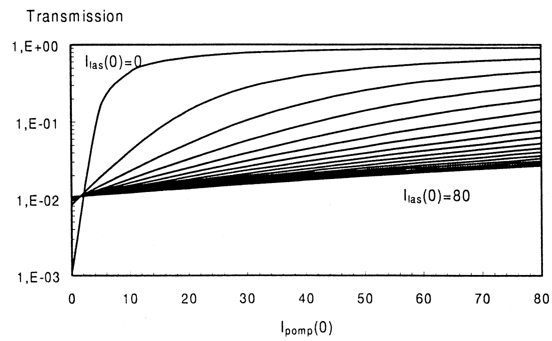

Fig. 4. Saturation of the reflection versus input pump intensity for input laser intensity varying in step of 5.

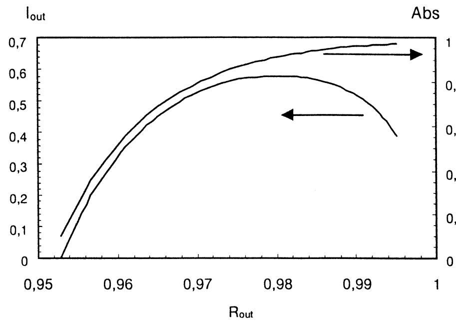

Fig. 5. Laser output intensity (left scale) and pump intensity absorption (right scale) as a function of the front face mirror reflectivity R_{out} for a 1 mm long YVO_4 crystal longitudinally pumped with an input pump intensity of 70.

the output mirror reflectivity. Then, we can plot the output intensity:

$$I_{out} = \frac{1-R_{out}}{R_{out}} I_{las}(0) = (G-1)\, I_{las}(0)$$

versus R_{out} $(1/G)$ where $I_{las}(0)$ is the laser intensity reflected by the output mirror. Such a curve appears in Fig. 5 for a 1 mm long crystal and a launched pump intensity of 70. On Fig. 5, the fraction of the absorbed pump intensity is also plotted.

Last, we compute the round trip gain at high injected laser intensity $(I_{las}(0)=80)$ for various pump intensities as a function of the amplifier length L_{amp}. The results appear in Fig. 6 showing that for large amplifier lengths, as the pump is totally absorbed, the laser wave is absorbed at a same rate than without pumping.

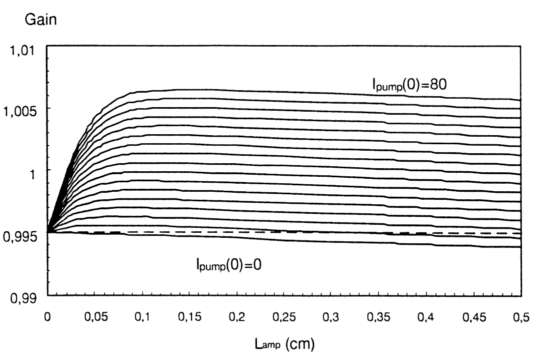

Fig. 6. Round trip gain versus crystal length with a pump intensity varying in steps of 5 for $I_{las}(0)=80$.

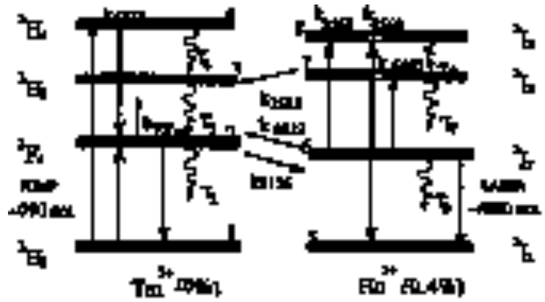

Fig. 7. Diagram of the lower energy manifolds and atomic transitions of a co-doped Tm,Ho system.

3. Tm,Ho:YLF amplifier

Identical computations may be performed for a codoped Tm,Ho amplifier. The relevant energy levels and atomic transitions are shown in Fig. 7. Amplification and absorption are described by [10]:

$$\frac{\mathrm{d}I_l^{\varepsilon}(z)}{I_l^{\varepsilon}(z)} = \varepsilon g_0\{X_6 - f\}\,\mathrm{d}z$$
$$\frac{\mathrm{d}I_p^{\varepsilon'}(z)}{I_p^{\varepsilon'}(z)} = -\varepsilon'\alpha_0\{1-X_2\}\,\mathrm{d}z \qquad (6)$$

with

$$g_0 = \sigma_l N_{Ho}(f_u + f_l), \quad \alpha_0 = \sigma_p N_{Tm}$$

$$X_6 = \frac{N_6}{N_{Ho}}, \quad X_2 = \frac{N_2}{N_{Tm}}$$

where N_K is the thulium $(K=\mathrm{Tm})$ and holmium $(K=\mathrm{Ho})$ doping concentration, and N_i is the population density for level 2 of thulium $(i=2)$ and level 6 of holmium $(i=6)$, respectively.

Introducing the energy transfer parameter θ between the $^3F_4$ level of the Tm^{3+} ion and the $^5F_7$ level of the Ho^{3+} ion [8]:

$$\theta = \frac{X_6}{X_2}\frac{1-X_2}{1-X_6}$$

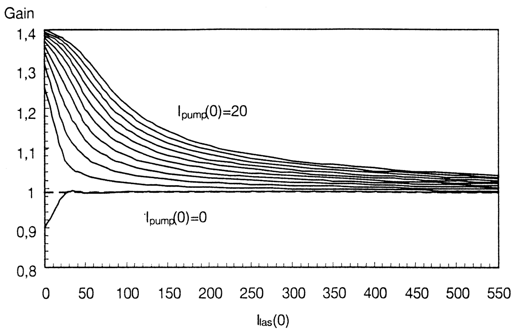

Fig. 8. Saturation of the round trip gain versus the input laser intensity for the input pump intensity varying in steps of 2. The YLF crystal length is 2.5 mm.

the amplification of the laser wave then reads:

$$\frac{\mathrm{d}I_1^{\varepsilon}(z)}{I_1^{\varepsilon}(z)} = \varepsilon g_0 \left\{ \frac{\theta X_2}{1+(\theta-1)X_2} - f \right\} \mathrm{d}z \tag{7}$$

According to [8], θ reads:

$$\theta = \frac{\sum\limits_{i\in {}^5I_7} g_i \exp\left(-\dfrac{E_i}{k_B T}\right)}{\sum\limits_{j\in {}^5I_8} g_j \exp\left(-\dfrac{E_j}{k_B T}\right)} \frac{\sum\limits_{k\in {}^3H_6} g_k \exp\left(-\dfrac{E_k}{k_B T}\right)}{\sum\limits_{l\in {}^3F_4} g_l \exp\left(-\dfrac{E_l}{k_B T}\right)} \tag{8}$$

where k_B is the Boltzmann constant, T is the temperature, and g_i the degeneracy of level i. Resolving the rate equation system in CW regime, the density of the Tm ions excited on the $^3F_4$ level is given by the equation [10]:

$$\begin{aligned} &-\frac{b}{2}(\theta-1)X_2^3 - \left\{ \frac{b}{2} + \left(I_p(z)+1\right)(\theta-1) \right. \\ &\left. + A\tau_2 N_{Ho}\theta \right\} X_2^2 - \left\{ I_p(z)(2-\theta) \right. \\ &\left. + I_l(z)\, r\rho(\theta - f(\theta-1)) + r\rho\theta + 1 \right\} X_2 \\ &+ I_p(z) + fr\rho I_l(z) = 0 \end{aligned} \tag{9}$$

where $r=(N_{Ho}/N_{Tm})$, $\rho=(\tau_2/\tau_6)$, τ_i is the spontaneous decay time of levels $^3F_4$ of the thulium ion ($i=2$) and $^5F_7$ of the holmium ion ($i=6$), and A is a constant relative to the energy transfer process between levels $^3F_4 \to {}^3H_6$ of Tm and $^5I_7 \to {}^5I_5$ of Ho. On the other hand, suppressing X_2 between the Eqs. (6) and (7) and assuming:

$$\xi \frac{\theta-1}{\theta} \frac{\mathrm{d}I_1^{\varepsilon}(z)}{g_0 I_1^{\varepsilon}(z)\,\mathrm{d}z} \ll 1$$

with

$$\xi = \frac{1}{1 - f\dfrac{\theta-1}{\theta}}$$

which is always verified [10], the pump absorption and the laser amplification are connected by a relation identical to the relation (4b) with:

$$D = \frac{\alpha_0}{g_0}\frac{\xi^2}{\theta}, \quad \delta = \alpha_0 \xi (1-f)$$

For a 6% Tm, 0.4% Ho codoped YLF crystal at 15°C, the constants are:

$$g_0 = 0.94\ \mathrm{cm}^{-1}, \quad \alpha_0 = 5.4\ \mathrm{cm}^{-1}$$

$$b = 54, \quad A = 12\times10^{-18}\ \mathrm{cm}^3/\mathrm{s}, \quad \theta = 18$$

$$r = 0.067, \quad \rho = 2$$

$$\tau_2 = 12\ \mathrm{ms}, \quad f = 0.21$$

The laser and pump saturation intensities are:

$$I_{sat}^{l} = 0.97\ \mathrm{kW/cm}^2, \quad I_{sat}^{p} = 1.63\ \mathrm{kW/cm}^2$$

In [10], the laser intensity reflected by the coupling mirror inside the laser amplifier 98% in reflectivity

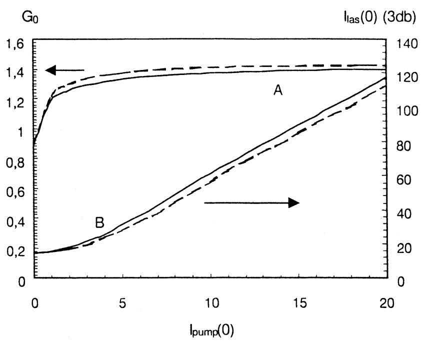

Fig. 9. Saturation of the small signal round trip gain (curve A) and input laser intensity required for a 3 dB reduction (curve B) versus the input pump intensity with (solid line) and without (dashed line) up-conversion.

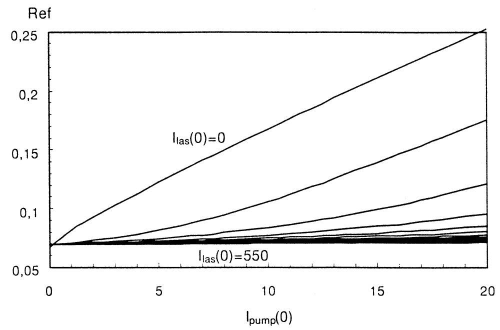

Fig. 10. Saturation of the reflection versus input pump intensity for input laser intensity varying in steps of 25.

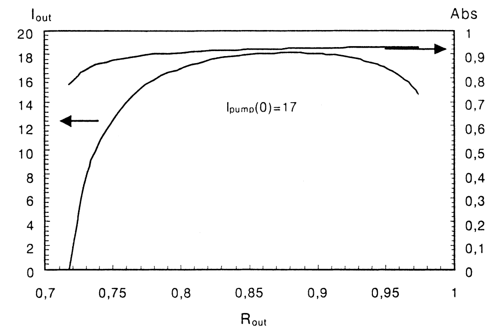

Fig. 12. Laser output intensity (left scale) and pump intensity absorption (right scale) as a function of the front face mirror reflectivity R_{out} for a 2.5 mm long YLF crystal longitudinally pumped with an input pump intensity of 17.

is 540 for a pump intensity of 17. Fig. 8 presents the saturation of the round trip gain versus the injected laser signal intensity $I_{las}(0)$ for various launched pump intensities $I_{pump}(0)$ varying from 0 to 20 in steps of 2 for a crystal length of 2.5 mm. In Fig. 9 the small signal gain (curve A solid line) and the injected laser intensity leading to a 3 dB attenuation of the small signal gain (curve B solid line) are plotted. Fig. 10 presents the saturation of the reflectivity versus the launched pump intensity $I_{pump}(0)$ showing that this reflectivity is 25% when no lasing and falls down to 7% for an injected laser intensity of 550. By neglecting up-conversion, we find that the gain does not change drastically (Fig. 9 dashed line) but the absorption at low laser intensity varies from 75% for $b = 54$ to 48% for $b = 0$. The reflectivity of the pump intensity versus the injected laser intensity is plotted in Fig. 11 for an input pump power equal to 10 and 20 with (solid line) and without (dashed line) up-conversion. For high laser and pump intensity, the results are quite comparable. As the upper laser level does not depopulates by up-conversion process, the absorption is lower and the gain greater. Then, the pump power is more efficiently converted into gain. On the other hand, at high laser intensity, the upper laser level depopulates fast reducing thereby the up-conversion efficiency.

Last, we present in Fig. 12 the output intensity and the corresponding pump intensity absorption versus the front face mirror reflectivity for a microlaser 2.5 mm in length for a pump intensity equal to 17. This last curve shows that our microlaser described in [10] with a 98% coupling is largely over coupled and then, the transverse mode operation discussed in [11] seems to not be surprising. As for the Tm:YVO_4 amplifier, we have also plotted in Fig. 13, the saturation of the gain for $I_{las}(0) = 550$ versus

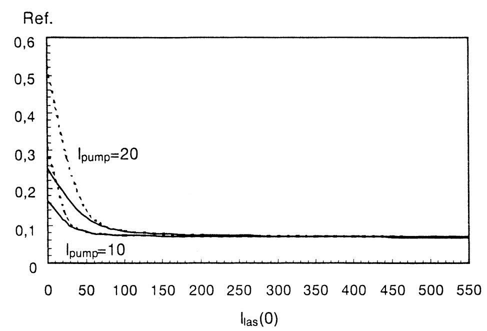

Fig. 11. Pump intensity reflection for $I_{pump}(0)$ equal to 10 and 20 with (solid line) and without (dashed line) up-conversion.

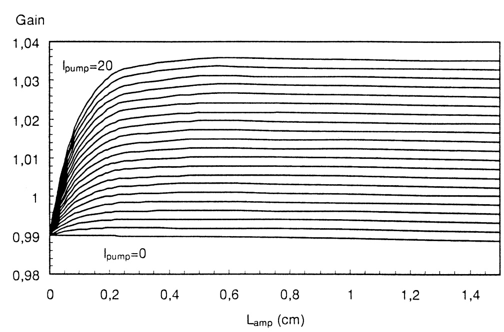

Fig. 13. Round trip gain versus crystal length with a pump intensity varying in steps of 1 for $I_{las}(0) = 550$.

the amplifier length that shows the limitation of the medium length when longitudinally pumped.

4. Amplification of a Gaussian laser beam

We now investigate the round trip amplification of a small signal Gaussian laser beam when a Tm,Ho:YLF amplifier is pumped by a Gaussian pump beam. We analyse the performances supplied by the amplifier in both power gain and beam quality when the ratio of the pump and the laser beam waist size w_p/w_l is varied. In these computations, we do not take into account of neither the diffraction nor the thermal induced self-focusing. The amplified beam is characterised by the M^2 beam quality factor and the spot size. Assuming a plane amplified wave, these parameters read:

$$M^2 = 2\pi\sigma_\rho\sigma_p = \frac{1}{2}\frac{\left\{\int_0^{2\pi}\int_0^{\infty} I_{amp}(\rho)\,\rho^3\,d\rho\,d\Phi \int_0^{2\pi}\int_0^{\infty}\frac{1}{I_{amp}(\rho)}\left(\frac{dI_{amp}(\rho)}{d\rho}\right)^2 \rho\,d\rho\,d\Phi\right\}^{\frac{1}{2}}}{\int_0^{2\pi}\int_0^{\infty} I_{amp}(\rho)\,\rho\,d\rho\,d\Phi} \tag{10}$$

$$W_0 = \sqrt{2}\,\sigma_p = \left\{2\frac{\int_0^{2\pi}\int_0^{\infty} I_{amp}(\rho)\,\rho^3\,d\rho\,d\Phi}{\int_0^{2\pi}\int_0^{\infty} I_{amp}(\rho)\,\rho\,d\rho\,d\Phi}\right\}^{\frac{1}{2}} \tag{11}$$

where σ_ρ and σ_p are the variances in the spatial and the spatial–frequency domain, respectively, and $I_{amp}(\rho)$ is the normalised intensity distribution of the amplified beam.

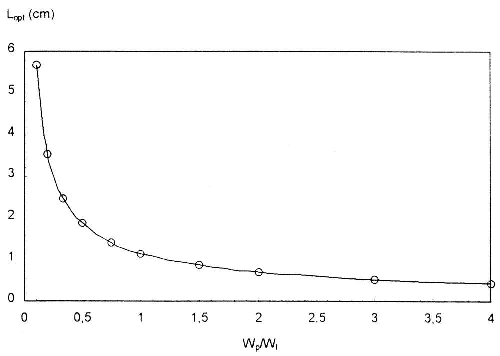

Fig. 14. Amplifier length for optimum intensity gain versus the ratio of the beam waist sizes of the pump and of the injected beam.

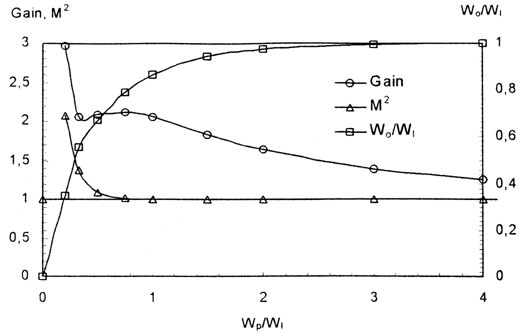

Fig. 15. Power gain (circles, left scale), M^2 factor (triangles, left scale) and W_0/w_l (squares, right scale) versus the ratio of the beam waist sizes of the pump and of the injected beam.

We assume a constant pump power and we choose:

$$I_{pump}(0)\,w_p^2 = 20$$

where $I_{pump}(\rho)$ is normalised intensity distribution of the pump beam. As shown in the former section, the amplifier length leading to an optimum intensity gain depends upon both the laser and the pump intensities. In a first step, we have computed this optimum length assuming $I_{las}(0) = 1$ as a function of w_p/w_l. The results are plotted on Fig. 14. Fig. 15 shows the power gain, the M^2 factor and W_0/w_l versus the ratio w_p/w_l. A maximum power gain of 2 with a M^2 factor of 1.01 is achieved with $w_p/w_l = 0.75$ and an amplifier length of 1.4 cm. We note that for higher injected signal intensity, as the gain saturates, the beam quality is improved. In Table 1, the optimum amplifier length, the power gain, the M^2 and W_0/w_l are reported for $w_p/w_l = 1$, $I_{las}(0) = 1$, 20 and 100.

The same computations have been performed for a constant pump intensity of 10 over a circle $3w_l$ in radius. The corresponding results appear in Table 2.

Table 1

$I_{las}(0)$	L_{opt} (cm)	$G(P)$	M^2	W_0/w_l
1	1.16	2.06	1.0025	0.87
20	0.75	1.55	1.0018	0.94
100	0.55	1.20	1.0010	0.98

Table 2

$I_{las}(0)$	L_{opt} (cm)	$G(P)$	M^2	W_0 / w_1
1	1	2.20	1.00006	1.008
20	0.6	1.66	1.0019	1.040
100	0.55	1.30	1.0017	1.071

As expected, the amplification is more efficient for a flat pump beam than for a Gaussian pump beam at constant pump power. However, as the intensity gain increases at the periphery of the laser beam, the amplified beam is wider than the injected beam and the beam quality is slightly reduced.

5. Conclusion

We have given, for the first time, a detailed calculation of the saturation coupling between gain and absorption in Tm:YVO_4 and Tm,Ho:YLF amplifier medium and investigated the effect of up-conversion process. These results are fruitful for laser design purposes and should be applicable also to other material if the various parameters are known. We have also investigated the amplification when both the laser and the pump beams are Gaussian and shown that the maximum power gain with low beam distortion is limited for longitudinal pumping. Then, as the pump wave is weakly absorbed in the regions where the laser intensity is low, side pumping of a power amplifiers fed by an end pumped master oscillator seems to be an efficient way for getting both high intensity levels and good mode quality. This scheme may also be investigated using the same model.

References

[1] P. Laporta, S. Taccheo, S. Longhi, O. Svelto, G. Sacchi, Single mode microchip Er-Yb:glass laser, Opt. Lett. 18 (1993) 1232–1234.

[2] W.L. Barnes, P.R. Morkel, L. Reekie, D.N. Payne, High-quantum efficiency Er^{3+} fiber laser pumped at 980 nm, Opt. Lett. 14 (1989) 1002–1004.

[3] N.S. Mishioka, Y. Damakevitz, Comparison of tissue ablation with pulsed Holmium and Thulium lasers, IEEE J. Quantum Electron. 26 (1990) 2271–2275.

[4] C. Hauglie-Hanssen, N. Djeu, Further investigations of a 2-μm Tm:YVO_4 laser, IEEE J. Quantum Electron. 30 (1994) 275–279.

[5] B.T. McGucking, R.T. Menzies, Efficient CW diode-pumped Tm,Ho:YLF laser with tunability near 2.067 μm, IEEE J. Quantum Electron. 28 (1992) 1025–1028.

[6] N.P. Barnes, E.D. Filer, C.A. Morrison, C.J. Lee, Ho:Tm lasers I: Theoretical, IEEE J. Quantum Electron. 32 (1996) 92–103.

[7] C.J. Lee, G. Han, N.P. Barnes, Ho:Tm lasers I: Experiments, IEEE J. Quantum Electron. 32 (1996) 105–111.

[8] G. Rustad, K. Stenersen, Modeling of laser-pumped Tm and Ho lasers accounting for upconversion and ground-state depletion, IEEE J. Quantum Electron. 32 (1996) 1645–1655.

[9] G.L. Bourdet, G. Lescroart, Theoretical modelling and design of a Tm:YVO_4 microchip laser, Opt. Commun. 149 (1998) 404–414.

[10] G.L. Bourdet, G. Lescroart, Theoretical modeling and design of a Tm, Ho:YLF microchip laser, Appl. Opt. 38 (1999) 3275–3281.

[11] G.L. Bourdet, G. Lescroart, R. Muller, Spectral characteristics of 2 μm microchip Tm:YVO_4 and Tm, Ho:YLF lasers, Opt. Commun. 150 (1998) 141–146.